

A Simple Model to Determine the Trends of Electric Field Enhanced Water Dissociation in a Bipolar Membrane*

XU Tongwen(徐铜文)^{a,b,**}, YANG Weihua(杨伟华)^a and HE Binglin(何炳林)^c

^aDepartment of Applied Chemistry; ^bResearch Center for Resources and Environments, University of Science and Technology of China, Hefei 230026, China

^cThe State Key Laboratory of Functional Polymeric Materials for Adsorption and Separation, Nankai University, Tianjin 300071, China

Abstract This work is concentrated on elucidating the mechanism of the electric field enhanced water dissociation. A simple model was established for the theoretical current-voltage characteristics in water dissociation process on a bipolar membrane based on the existence of a depletion layer and Onsager's theory. Particular attention was given to the influence of applied voltage on depletion thickness and the dissociation constant. The factors on the water splitting process, such as water diffusivity, water content, ion exchange capacity, temperature, relative permittivity, etc. were adequately analysed based on the derived model equations and several suggestions were proposed for decreasing the applied voltage in practical operation. The water dissociation tests were conducted and compared with both the theoretical calculation and the measured current-voltage curves reported in the literature, which showed a very good prediction to practical current-voltage behavior of a bipolar membrane at high current densities when the splitting of water actually commenced.

Keywords bipolar membrane, electric field, water dissociation, current-voltage characteristics

1 INTRODUCTION

A bipolar membrane (BM) is composed of a cation (with negatively fixed charge) and an anion ion-exchange layer (with positively fixed charge) joined together in series. Just the same as the discovery of N-P junctions in the semiconductor technology, this composition brings about many novelties to a bipolar membrane, making it useful in many new technological applications^[1-4], most of which originate from its ability to dissociate water when high reverse voltage is applied. Its potential as a water-splitting technology has attracted many investigations. But the actual mechanism causing this splitting remains a matter of controversy and at present no model can explain completely all the phenomena existing in a water dissociation process^[5,6]. Up to now, three physical models have been proposed: second Wien effect model(SWEM)^[7], chemical reaction model(CRM)^[8] and neutral layer model(NLM)^[9], providing a theoretical basis to investigate this water dissociation process. Theories based on these models have explained some particular experimental phenomena to some extent. However, among them, SWEM seems to be most widely accepted^[10,11]. This model assumed that there is a dry "space charge region"^[12] or "depletion layer"^[13] at the transition layer (TRL), i.e. the junction between the cation and anion layers, where the mobile ions have much smaller concentrations than

the fixed charge^[10-14]. When high reverse voltage is applied, just as the same as that in a double-layer biological membrane containing fixed charge and exhibiting rectification and capacitance properties, water dissociation occurs mainly at this zone and behaves as a weak electrolyte. Theories based on these assumptions allowed for reasonable explanation of experimental facts^[10,11,14-19]. The existence of a depletion layer at the junction is also supported by the recent investigations in terms of the measurements of AC conductance at low frequency^[20]. But the existing models for water dissociation were derived from the viewpoint of physics and most derivations were based on steady state process^[3,4,8-12,14-16,17-19].

The work described here is concentrated on elucidating the mechanism of the electric field enhanced water dissociation. A simple model was derived to describe the voltage-current characteristics base on both SWEM^[7] and Space Charge Theory^[12] from the viewpoint of chemical engineering (equation of continuity) and unsteady state. Furthermore, theory and calculation are compared with the measured current-voltage curves and those reported by Strathmann *et al.*^[6].

2 MODEL AND BASIC EQUATIONS

A bipolar membrane considered here consists of an anion and a cation selective layer joined together with a transition layer (TRL) at the junction when an elec-

Received 2000-01-23, accepted 2000-08-31.

* Supported by the National Natural Science Foundation of China (No. 29976040), the Natural Science Foundation of Anhui Province (No. 99045431) and Youth Foundation of USTC.

** To whom correspondence should be addressed. E-mail: twxu@ustc.edu.cn

tric field is established across the membrane. As depicted in Fig. 1, the thickness of anionic and cationic exchange layers is d_m^A and d_m^C , and the fixed charge concentration of the two layers is X_m^A and X_m^C , respectively. The transition layer is depleted of ions and has a total thickness of $\lambda = \lambda_N + \lambda_P$, where λ_N and λ_P correspond the depletion thickness in the negatively and positively charged layers. To develop the present model, the following assumptions which were shown to be reasonable^[6,7,10,11,16-19], are adopted in this paper.

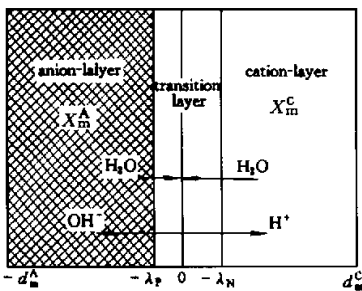
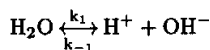


Figure 1 Schematic drawing demonstrating the function and structure of a bipolar membrane

(1) Water dissociation mainly occurs in the transition or depletion layer and the dissociated ions removed from this region are replenished by the following water dissociation equilibrium



(2) The water dissociation is accelerated by the electric field according to the second Wien effect which describes the influence of a strong electric field on water dissociation constant k_1 while the recombination rate constant k_{-1} is not effected by the electric field.

(3) The generated protons and hydroxyl ions are removed from the transition region by migration and the consumed water can be compensated timely by diffusion from the bulk solution.

(4) The electric current is calculated from the migration flux of either protons or hydroxyl ions.

(5) The voltage drops across both anion and cation exchange layers are neglected so that voltage across a bipolar membrane is equal to that across the transition region and the driving force for the migration of ions is U^{tr}/λ , since the Donnan potential is in equilibrium with the diffusion of ions into the transition region.

A simplified schematic diagram of species transport into or from the transition layer(TRL) is illustrated in Fig. 1. Using the equation of continuity, the

following equation is established

$$\lambda \frac{dc_j^{tr}}{dt} = (J_{j,diff} - J_{j,mig}) + \lambda r_j, \quad j = H^+, OH^-, H_2O \quad (1)$$

Here r_j are the reaction rates of the protons, hydroxyl ions and water in the transition region which are expressed as

$$r_{H^+} = r_{OH^-} = -r_{H_2O} = k_1 c_{H_2O} - k_{-1} c_{H^+} c_{OH^-} \quad (2)$$

Within the model, the diffusion water transport fluxes into the anion layer (A) and the cation layer(C) are described by Fick's law

$$J_{H_2O,diff}^A \cong D_{H_2O}^A \frac{c_{H_2O}^A - c_{H_2O}^{tr}}{d_m^A} \quad (3)$$

$$J_{H_2O,diff}^C \cong D_{H_2O}^C \frac{c_{H_2O}^C - c_{H_2O}^{tr}}{d_m^C} \quad (4)$$

where the water concentration in the both layers is assumed to be linear for simplicity^[6,21]. The migration of protons and hydroxyl ions is calculated with the Nernst-Planck equation

$$J_{H^+,mig} = u_{H^+}^{tr} c_{H^+}^{tr} \frac{U^{tr}}{\lambda} \quad (5)$$

$$J_{OH^-,mig} = u_{OH^-}^{tr} c_{OH^-}^{tr} \frac{U^{tr}}{\lambda} \quad (6)$$

where $u_{H^+}^{tr}$, $u_{OH^-}^{tr}$, $c_{H^+}^{tr}$, $c_{OH^-}^{tr}$ are the respective mobilities and concentrations of protons and hydroxyl ions in the transition layer. Substituting Eqs.(2)–(6) into Eq.(1) yields the concentration change of different species in the transition layer

$$\frac{dc_{H^+}^{tr}}{dt} = k_1 c_{H_2O}^{tr} - k_{-1} c_{H^+}^{tr} c_{OH^-}^{tr} - \frac{u_{H^+}^{tr} c_{H^+}^{tr}}{\lambda} \frac{U^{tr}}{\lambda} \quad (7)$$

$$\frac{dc_{OH^-}^{tr}}{dt} = k_1 c_{H_2O}^{tr} - k_{-1} c_{H^+}^{tr} c_{OH^-}^{tr} - \frac{u_{OH^-}^{tr} c_{OH^-}^{tr}}{\lambda} \frac{U^{tr}}{\lambda} \quad (8)$$

$$\begin{aligned} \frac{dc_{H_2O}^{tr}}{dt} = & k_{-1} c_{H^+}^{tr} c_{OH^-}^{tr} - k_1 c_{H_2O}^{tr} + \\ & \frac{D_{H_2O}^A}{\lambda} \frac{c_{H_2O}^A - c_{H_2O}^{tr}}{d_m^A} + \frac{D_{H_2O}^C}{\lambda} \frac{c_{H_2O}^C - c_{H_2O}^{tr}}{d_m^C} \end{aligned} \quad (9)$$

Based on assumption (2), k_1 is enhanced by the applied electric field and follows the SWE model

$$\frac{k_1}{k_1^0} = 1 + b + \frac{b^2}{3} + \frac{b^3}{18} + \frac{b^4}{180} + \frac{b^5}{2700} + \frac{b^6}{56700} + \dots \quad (10)$$

with

$$b = 0.09636 \frac{E}{\epsilon_r T^2} \quad (11)$$

where ϵ_r is the relative permittivity, k_1 is the forward rate constant of the net reaction responsible for the

electric field enhanced water dissociation as described in Eq. (2) and k_1^0 is the forward rate constant of the reaction when no external electric field is applied. For a bipolar membrane water dissociation process, E can be as high as $10^8 \text{ V}\cdot\text{m}^{-1}$ [19], b is generally greater than 3[9], and thus Eq. (10) can be simplified to[6,9,17]

$$\frac{k_1}{k_1^0} = \left(\frac{2}{\pi}\right)^{\frac{1}{2}} (8b)^{-\frac{3}{2}} \exp(8b)^{\frac{1}{2}} \quad (12)$$

Based on the Poisson equation, the electric field density E and the total depletion thickness can be related to the potential drop applied in the depletion layer, U^{tr} , as follows[10,12,17,19]

$$E = \left[\frac{2F}{\epsilon_r \epsilon_0} U^{\text{tr}} \frac{X_m^A X_m^C}{X_m^A + X_m^C} \right]^{1/2} \quad (13)$$

$$\lambda = \lambda_N + \lambda_P = \left[\frac{2\epsilon_r \epsilon_0}{F} U^{\text{tr}} \frac{X_m^A + X_m^C}{X_m^A X_m^C} \right]^{1/2} \quad (14)$$

Here, F is the Faraday constant. According to assumption (2), the electric current density can be calculated from the hydroxyl ion or proton flux as follows

$$I = F u_{\text{OH}^-}^{\text{tr}} - c_{\text{OH}^-}^{\text{tr}} \frac{U^{\text{tr}}}{\lambda} = F u_{\text{H}^+}^{\text{tr}} + c_{\text{H}^+}^{\text{tr}} \frac{U^{\text{tr}}}{\lambda} \quad (15)$$

This is the final form of current-voltage characteristics. Though the form of this equation is consistent with most literatures, in our equation $c_{\text{H}^+}^{\text{tr}}$ is no longer assumed as a constant and will change with the applied voltage, time and membrane properties as described in Eqs. (7)–(9). Considering that the concentrations of protons and hydroxyl ions and depletion thickness will change with the applied voltage, the theoretical potential drop across a bipolar membrane should be non-linearly related to the current density applied, which is consistent with the most experimental phenomena[6,21,22].

3 RESULTS AND DISCUSSION

3.1 Results from the model calculations

For a bipolar membrane water dissociation process, the unsteady state occurs only at the very beginning (about 10^{-4} s) [6]. Thus the steady state is reasonably assumed and the left side of Eqs. (7)–(9) are set to zero. Rearranging these equations yields the following quadratic equation on the concentration of protons

$$k_{-1}(c_{\text{H}^+}^{\text{tr}})^2 + \left(k_1 + \frac{2D_{\text{H}_2\text{O}}}{\lambda d_m} \right) \frac{u_{\text{H}^+}^{\text{tr}} U^{\text{tr}}}{\lambda} - \frac{d_m}{2D_{\text{H}_2\text{O}}} c_{\text{H}^+}^{\text{tr}} - k_1 c_{\text{H}_2\text{O}} = 0 \quad (16)$$

where the characteristic parameters of both anion and cation layers are assumed to be identical, i.e., $D_{\text{H}_2\text{O}}^C = D_{\text{H}_2\text{O}}^A$, $c_{\text{H}_2\text{O}}^C = c_{\text{H}_2\text{O}}^A = c_{\text{H}_2\text{O}}$, $X_m^C = X_m^A = X$, $d_m^C = d_m^A = d_m$, $u_{\text{H}^+}^{\text{tr}} = u_{\text{OH}^-}^{\text{tr}}$. The concentration of H^+ in transition layer can be easily obtained.

Figure 2 demonstrates the effect of fixed group concentration (X) on the calculated I - U curves by substituting the typical parameters as shown in Table 1. Obviously, with the increasing fixed group concentration, water dissociation speeds up and thus the water concentration in the transition zone is decreased due to the increasing consumption of water as shown in Fig. 3.

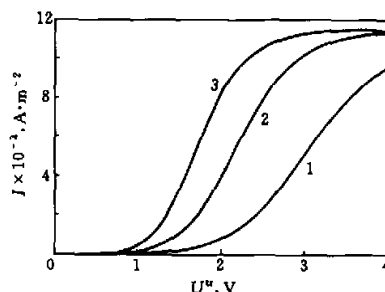


Figure 2 Influence of fixed group concentration on the I - U curves
 X , $\text{mol}\cdot\text{m}^{-3}$: 1—1000; 2—1500; 3—2000

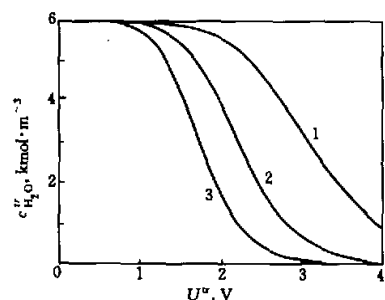


Figure 3 Influence of fixed group concentration on the water concentration in the transition layer
 X , $\text{mol}\cdot\text{m}^{-3}$: 1—1000; 2—1500; 3—2000

The effects of water diffusivity on the dissociation rate are illustrated in Figs. 4 and 5. Water concentration in TRL decreased when the diffusion coefficient of water in the membrane is decreased. Because at this case, water flux into TRL decreases and the water, which has been dissociated into protons and hydroxyl ions, can not be compensated by the water transported into the membrane due to diffusion, and thus cause a decrease in water concentration therein. As shown in Eqs. (7) and (8), the concentration of protons and hydroxyl ions depend on the water concentration and will decrease with a decrease in water

Table 1 The typical parameters used for calculations

Parameter	Value	Source
Faraday constant, F	$96486 \text{ A}\cdot\text{s}\cdot\text{mol}^{-1}$	
permittivity of free space, ϵ_0	$8.85 \times 10^{-12} \text{ A}\cdot\text{s}\cdot\text{V}^{-1}\cdot\text{m}^{-1}$	universal constants
dissociation rate constant k_1^0	$2 \times 10^{-5} \text{ s}^{-1}$	
combination rate constant k_{-1}	$1.1 \times 10^8 \text{ m}^3\cdot\text{mol}^{-1}\cdot\text{s}^{-1}$	
mobility of protons in TRL, u_{H}^{tr}	$30.0 \times 10^{-8} \text{ m}^2\cdot\text{V}^{-1}\cdot\text{s}^{-1}$	
mobility of hydroxyl ion in TRL, $u_{\text{OH}}^{\text{tr}}$	$30.0 \times 10^{-8} \text{ m}^2\cdot\text{V}^{-1}\cdot\text{s}^{-1}$	adapted from [6], [21], [23]
relative permittivity in TRL, ϵ_r	20	
initial concentration of proton and hydroxyl in TRL, $c_{\text{H}}^{\text{tr},0}, c_{\text{OH}}^{\text{tr},0}$	$10^{-4} \text{ mol}\cdot\text{m}^{-3}$ ($10^{-7} \text{ mol}\cdot\text{L}^{-1}$)	
concentration of water in BM, $c_{\text{H}_2\text{O}}^{\text{bm}}$	$6000 \text{ mol}\cdot\text{m}^{-3}$	
initial concentration of water in TRL, $c_{\text{H}_2\text{O}}^{\text{tr},0}$	$6000 \text{ mol}\cdot\text{m}^{-3}$	
temperature, T	293.15 K	
thickness of the layers, d	10^{-4} m	
diffusion coefficient of water in both layers, $D_{\text{H}_2\text{O}}$	$10^{-9} \text{ m}^2\cdot\text{s}^{-1}$	experimental determination
concentration of fixed groups, X	$1.5 \times 10^3 \text{ mol}\cdot\text{m}^{-3}$	

concentration in TRL. Thus the observable current density as calculated from Eq. (14) is also decreasing as shown in Fig. 5. It should be noted that if the water concentration in the TRL reaches a very small value, the water dissociation and hence the current density will be limited by the diffusion of water into the membrane. Therefore, in practical operations, a bipolar membrane with high water diffusivity is strongly recommended for enhancing water splitting and saving energy.

Water content in the membrane has the same posi-

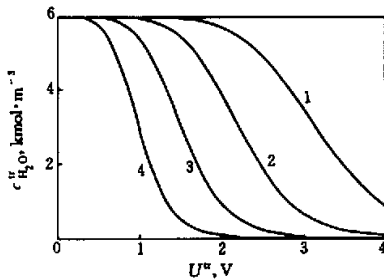


Figure 4 Influence of $D_{\text{H}_2\text{O}}$ on the water concentration in TRL

$D_{\text{H}_2\text{O}}, \text{m}^2\cdot\text{s}^{-1}$: 1— 10^{-8} ; 2— 10^{-9} ; 3— 10^{-10} ; 4— 10^{-11}

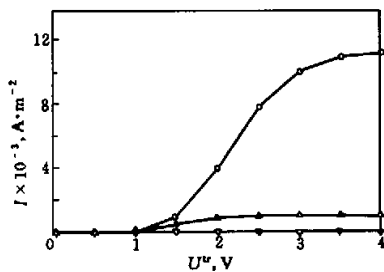


Figure 5 Influence of $D_{\text{H}_2\text{O}}$ on the current-voltage curve

$D_{\text{H}_2\text{O}}, \text{m}^2\cdot\text{s}^{-1}$: \circ — 10^{-8} ; \triangle — 10^{-10} ; ∇ — 10^{-11}

tive effect as water diffusivity. As shown in Fig. 6, with the increasing content of water contained initially in the membrane, decline of the rate of water concentration in TRL will be slowed down. Just as observed in Fig. 7, the water concentration in TRL will increase at the same voltage applied, and thus the current density increases and water dissociation is favorable.

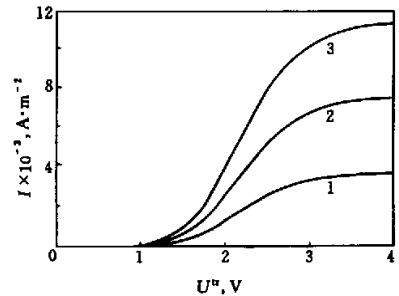


Figure 6 Influence of initial water concentration in the membrane on the current-voltage curve

$c_{\text{H}_2\text{O}}^{\text{bm}}, \text{mol}\cdot\text{m}^{-3}$: 1—2000; 2—4000; 3—6000

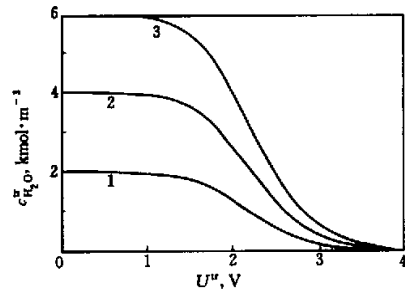


Figure 7 Influence of initial water concentration in the membrane on that in the transition layer

$c_{\text{H}_2\text{O}}^{\text{bm}}, \text{mol}\cdot\text{m}^{-3}$: 1—2000; 2—4000; 3—6000

Figure 8 demonstrates the current-voltage curves for water dissociation using a bipolar membrane, computed for different temperatures. Typical parameters

as shown in Table 1 have been used in calculation. It is obvious that water-splitting effects is enhanced as temperature increases. This enhancement of electric current is vague from model Eqs. (10)–(14), but it can qualitatively explained by the classic relationship for the rate constants involved in each equation^[24]

$$k_1^0(T) = A \exp \left[- \frac{E_a}{RT} \right] \quad (17)$$

where A is the value of the rate constant at a reference temperature and E_a is the activation energy of the process and has a typical value of $106 \text{ kJ}\cdot\text{mol}^{-1}$ ^[25]. Therefore, an increase in the rate constant with temperature is observed based on Eqs. (11), (12) and (15) as depicted in Fig. 9. This may be mainly responsible for acceleration of water dissociation.

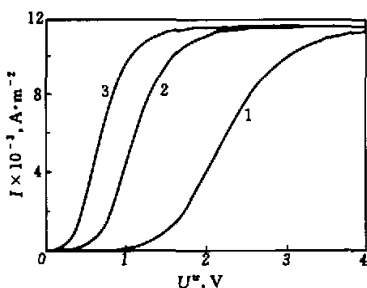


Figure 8 Influence of temperature on the current-voltage curve
 T, K: 1—293.15; 2—303.15; 3—333.15

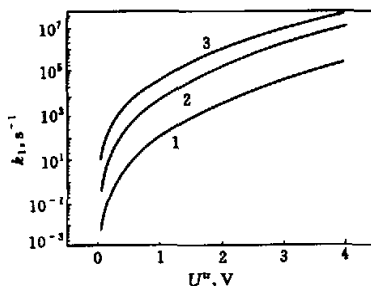


Figure 9 Influence of temperature on the water dissociation rate constant
 T, K: 1—293.15; 2—303.15; 3—333.15

Effect of relative permittivity is shown in Fig. 10. It can be seen that an increase in relative permittivity has the tendency to slow down water splitting. Appreciable accelerated water dissociation is observed only at the case that ϵ_r is less than about 10 because the rate constant is significant larger at low ϵ_r compared with that at high ϵ_r as shown in Fig. 11.

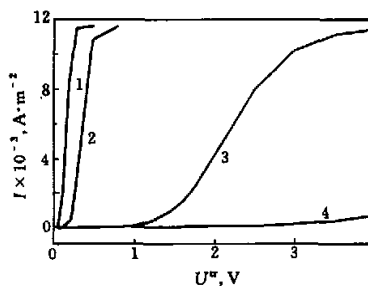


Figure 10 Influence of relative permittivity on the current-voltage curve
 ϵ_r : 1—9; 2—10; 3—20; 4—30

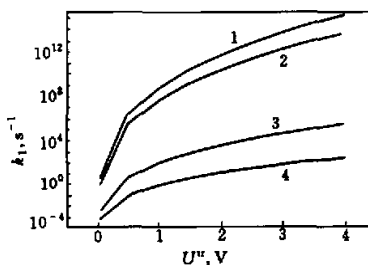


Figure 11 Influence of relative permittivity on the water dissociation rate constant
 ϵ_r : 1—9; 2—10; 3—20; 4—30

3.2 Verification of the derived models from the experimental observations

The theoretically calculated data and the measured current-voltage curves are shown in Figs. 12 and 13. The membrane in Fig. 12 is prepared in our lab which has nearly the same parameters as the typical ones^[26]. Obviously, the experimentally measured current densities are consistent with theoretical calculation. However, it should be noted that our model describes the electric current due to the water dissociation process (transport of water ions and the related reaction) and thus predicts the I - U curves quite well at relatively higher current densities. For further comparison, experimental data for the membrane denoted as bm1 from literature^[6] is used and the theoretical calculation was made under their experimental conditions. The result is shown in Fig. 13, indicating that our model can give fairly good prediction except certain deviation at high voltage region due to that the referred bm1 membrane has a relatively low water permeability.

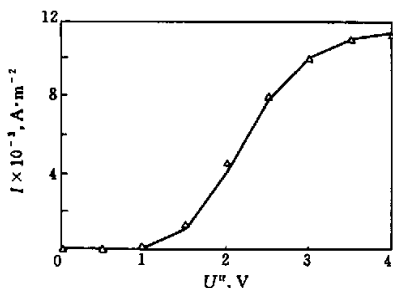


Figure 12 Calculated and measured I - U curves of a self-made bipolar membrane

($X = 1500$, $D_{\text{H}_2\text{O}} = 10^{-9}$, $d = 0.1$ nm and other parameters conformed to Table 1)

— theoretical; Δ experimental points^[26]

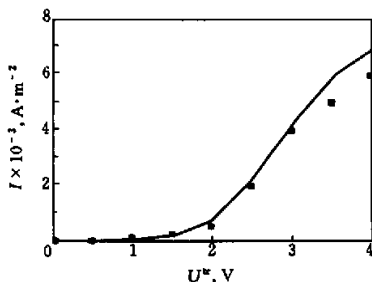


Figure 13 Comparison of the experimental and theoretical in literature for bm1 membrane

($X = 1000$, $D_{\text{H}_2\text{O}} = 5.5 \times 10^{-10}$, $d = 0.08$ nm and other parameters conformed to Table 1)

■ experimental^[6]; — calculated data

4 CONCLUSIONS

A simple model was established to describe the theoretical current-voltage relationship across bipolar membranes with both the transports of water ions and the reaction taken into consideration. Particular attention was given to the influence of applied voltage on water concentration in the transition layer and the dissociation constant. The factors on the water splitting process, such as water diffusivity, water content, ion exchange capacity, temperature, relative permittivity, *etc.* were adequately analysed based on the derived model. For practical applications, a bipolar membrane with proper ion exchange capacity, high water content, high permeability to water and a third layer which may be composed of amphiprotic hydroxide compounds or polymeric weak acid to decrease the relative permittivity is strongly recommended^[21]. Furthermore, operation at a relatively high temperature is also suggested.

The water dissociation tests were conducted and compared with both the theoretical calculation and the measured current-voltage curves reported in liter-

ature, which showed some consistence with a practical current-voltage behavior of a bipolar membrane at high current densities when the splitting of water actually commenced. However, uncertainty exists about the relative permittivity and deviation of the recommended membrane parameters from the practical measurements, more precise prediction to the experimental data seems to be difficult.

NOMENCLATURE

c	concentration for water and water ions, $\text{mol}\cdot\text{m}^{-3}$
D	diffusion coefficient, $\text{m}\cdot\text{s}^{-2}$
d	thickness, m
E	electrical field strength, $\text{V}\cdot\text{m}^{-1}$
F	Faraday constant, $96486 \text{ A}\cdot\text{s}\cdot\text{mol}^{-1}$
I	current density, $\text{A}\cdot\text{M}^{-2}$
J	flux, $\text{mol}\cdot\text{m}^{-2}\cdot\text{s}^{-1}$
R	gas constant, $8.314 \text{ J}\cdot\text{mol}^{-1}\cdot\text{K}^{-1}$
r	reaction rate
T	temperature, K
t	time, s
U	potential drop, V
u	mobility, $\text{cm}^2\cdot\text{s}^{-1}\cdot\text{V}^{-1}$
X	fixed group concentration of monolayer, $\text{mol}\cdot\text{m}^{-3}$
ϵ_0	permittivity of free space, $8.85 \times 10^{-12} \text{ A}\cdot\text{s}\cdot\text{V}^{-1}\cdot\text{m}^{-1}$
ϵ_r	relative permittivity
λ	depletion thickness, m

Superscripts

A	anion exchange layer
bm	bipolar membrane
C	cation exchange layer
tr	transition layer
0	initial value ($t = 0$)

Subscripts

H^+	protons
H_2O	water
diff	diffusion
j	species j
m	membrane phase
mig	migration
OH^-	hydroxyl ions

REFERENCES

- Xu, T. W., Wang, Zh. W., Liu, N., "Prospect of the theory and application for a bipolar membrane", *Water Treatment*, **24** (1), 20—25 (1998). (in Chinese)
- Tsuru, T., Nakao, S., Kimura, S., "Ion separation by bipolar membranes in reverse osmosis", *J. Membr. Sci.*, **108**, 269—278 (1995).
- Bauer, B., Gerner, F. J., Strathmann, H., "Development of bipolar membranes", *Desalination*, **68**, 279—292 (1988).
- Mani, K. N., "Electrodialysis water splitting technology", *J. Membr. Sci.*, **58**, 117—138 (1991).
- Simons, R., "Electric field effects on proton transfer between ionizable groups and water in ion exchange membranes", *Electrochim. Acta*, **29**, 151—158 (1984).
- Strathmann, H., Krol, J. J., Rapp, H. J., *et al.*, "Limiting current density and water dissociation in bipolar membranes", *J. Membr. Sci.*, **125**, 123—142 (1997).

- 7 Onsager, L., "Deviations from Ohm's Law in weak electrolytes", *J. Chem. Phys.*, **2**, 599—612 (1934).
- 8 Simons, R., "Strong electric fields effects on proton transfer between membrane-bound amines and water", *Nature*, **280**, 824—826 (1979).
- 9 Simons, R., Khanarian, G., "Water dissociation in bipolar membranes: Experiments and theory", *J. Membr. Biol.*, **38**, 11—30 (1978).
- 10 Holdik, H., Alcaraz, A., Ramirez, P., et al., "Electric field enhanced water dissociation at the bipolar junction from ac impedance spectra measurements", *J. Electroanalytical Chemistry*, **442**, 13—18 (1998).
- 11 Mafe, S., Ramirez, P., Alcaraz, A., "Electric field-assisted proton transfer and water dissociation at the junction of a fixed-charged bipolar membrane", *Chemical Physics Letters*, **294**, 406—412 (1998).
- 12 Mauro, A., "Space charge region in fixed charge membranes and the associated property of capacitance", *Biophysical J.*, **2**, 179—197 (1962).
- 13 Simons, R., "The steady and non steady state properties of bipolar membranes", *Biochim. Biophys. Acta*, **274**, 1—14 (1972).
- 14 Coster, H. G. L., "The double fixed charge membrane", *Biophysical J.*, **13**, 118—132 (1973).
- 15 Chilcott, T. C., Coster, H. G. L., George, E. P., "AC impedance of the bipolar membrane at low and high frequencies", *J. Membr. Sci.*, **100**, 77—86 (1995).
- 16 Coster, H. G. L., "A quantitative analysis of the voltage-current relationships of fixed charge membranes and the associated property of punch-through", *Biophysical J.*, **5**, 669—679 (1965).
- 17 Mafe, S., Manzanares, J. A., "Model for ion transport in bipolar membranes", *Phys. Rev. A*, **42**, 6245—6248 (1990).
- 18 Ramirez, P., Manzanares, J. A., Mafe, S., "Water dissociation effects in ion transport through anionic exchange membranes with thin cationic exchange surface films", *Ber. Bunsenges Phys. Chem.*, **95** (1), 499—503 (1991).
- 19 Simons, R. A., "Mechanism for water flow in bipolar membranes", *J. Membr. Sci.*, **82**, 65—73 (1993).
- 20 Smith, J. R., Simons, R., Weidenhaun, J., "The low frequency conductance of bipolar membranes demonstrates the presence of a depletion layer", *J. Membrane Sci.*, **140**, 155—164 (1998).
- 21 Xu, T. W., Yang, W. H., He, B. L., "Water dissociation phenomena in a bipolar membrane—the configurations and theoretical voltage analysis", *Science in China*, **42** (6), 589—598 (1999).
- 22 Simons, R., "Preparation of a high performance bipolar membrane", *J. Membr. Sci.*, **762**, 13—23 (1993).
- 23 Atkins, P. W., *Physical Chemistry*, 5th ed., Oxford University Press, Oxford, (1994).
- 24 Jordan, P. C., *Chemical Kinetics and Transport*, Plenum Press, New York (1979).
- 25 Ramire, P., Aguilera, V. M., Manzanares, J. A., et al, "Effect of temperature and ion transport on water splitting in bipolar membranes", *J. Membr. Sci.*, **73**, 191—201 (1992).
- 26 Xu, T. W., "Preparation of a homogeneous bipolar membrane and the water splitting mechanism therein", *Postdoctoral Report*, Nankai University, Tianjin (1997).